ON ATOMIZATION AND LINEARIZED FREE-SURFACE INSTABILITY ON ROTATING BODIES

by

A. M. DRUMMOND

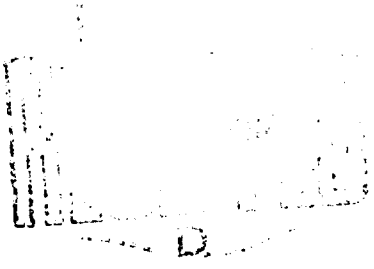

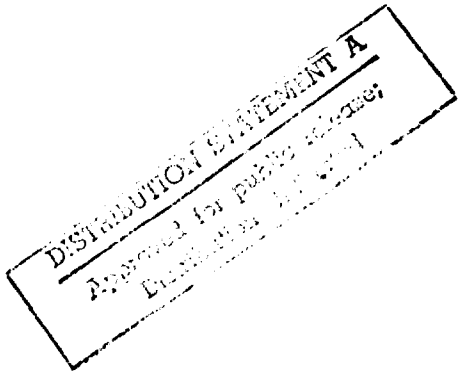

A. D. Wood, Head
Flight Research Section

F. R. Thurston
Director

SUMMARY

A surface-wave instability theory applicable to spinning discs and cups is presented and a new explanation of atomization from these devices is proposed. The theory predicts an unstable disturbance wavelength that correlates with experimental results of Hinze and Milborn for ligament formation from a rotating cup. The linear analysis is restricted to flows where perturbation amplitude is much less than film thickness.

TABLE OF CONTENTS

ILLUSTRATIONS

ILLUSTRATIONS (Cont'd)

SYMBOLS

Symbol	Definition
a^*	Circumference of rotating body
a	Amplitude of surface perturbation
C, C'	Constants
d	Drop diameter
D	Disc diameter
g	Acceleration of gravity
h, h'	Depths of fluid and air layers respectively
$\bar{h}$	h/r
k	$2\pi/\lambda$
K	Constant
P, P'	Pressure in fluid and air layers respectively
P_s, P'_s	Steady pressure at free-surface in fluid and air layers respectively
p, p'	Perturbation pressures in fluid and air layers respectively
Q	Flow rate
Re	Reynolds Number rV_r/ν
r	Radius from axis of rotation
r'	Perturbed free surface shape = $r+\eta$
r_c	Radius of curvature on circular arc edge
$\dot{r}$	Local body surface slope
S	ρ' coth kh'/ρ coth kh
T	Surface tension

SYMBOLS (Cont'd)

Symbol	Definition
t	Time
v_r	Radial velocity component
V_T, V_T'	Tangential velocities of fluid and air respectively
W	Weber Number $rV_T^2\rho/T$
y	Co-ordinate normal to free surface
z	Number of ligaments
α	Angle around circular arc edge
σ	$\gamma \pm i\delta$
ρ, ρ'	Density of fluid and air respectively. ($\rho' = .002378$ slugs/ft^3)
ϕ_1, ϕ_1'	Perturbation potentials of fluid and air respectively
η	Perturbation to free surface
λ	Disturbance wavelength
λ^*	$\lambda/2\pi r$
λ_1^*	Root of stability equation
λ_{CRIT}^*	Wavelength of fastest growing wave
μ	Absolute viscosity of liquid
ν	Kinematic viscosity of liquid
Ω	Angular velocity
θ	Azimuth angle around rotating body
∇^2	Laplacian Operator

ON ATOMIZATION AND LINEARIZED FREE-SURFACE INSTABILITY ON ROTATING BODIES

1.0 INTRODUCTION

Flow with a free-surface on rotating bodies is of interest in the study of rotary atomizers. Such devices find application in agriculture for dispensing insecticides and herbicides, in combustion research and furnaces for spraying fuel in a finely divided state into combustion chambers, and in spray-drying processes of many kinds.

The purpose of this paper is to develop a surface-wave instability theory to explain the process of atomization from spinning discs and cups. The motivation to do this rests on the proven surface instability of fluid ligaments and sheets and in the hope of showing a unified mechanism for the explanation of fluid atomization. No attempt is made to discuss drop-size distributions resulting from the atomization process and no new experimental data are presented. However, attempts at using existing experimental data to verify the theory are made.

The steady solution of Drummond[1] for the viscous flow with a free-surface on rotating bodies is used as a starting point and the work of Lamb[2] is used as the reference for the free-surface perturbation analysis.

Pedley[3] has studied the stability of rotating flows with a free surface where the free surface is cylindrical in form and can be either an "inner" or "outer" boundary. His linear analysis is limited to inviscid fluids with "large" depth in conjunction with "inertia-less" air. However, he derives sufficient and sometimes necessary conditions for stability by a method quite different from that of Lamb. Pedley provides an extensive list of references to free-surface instability. His results will be extended in this work to cover approximately viscous flows by Lamb's method and the two results will be shown to be compatible.

Consider the flow of a viscous fluid on a rotating disc (Fig. 1). The depth of the film varies with radius on the flat part of the disc and also with α on the circular arc edge. However, as long as α is a bit less than 90°, then the film is nearly of constant thickness on the edge. Figure 2 shows a typical thickness variation with r and α from Reference 1. Also, if the radius of curvature r_c of the circular arc edge is small, then the radius r to any point on the arc is nearly constant and is not a function of α. The velocity component v_r in the r direction gets very small on the edge, and the tangential velocity is the dominant component. Figure 3 shows typical values from Reference 1. The normal component is very much less than v_r. We wish to investigate surface waves on the circular arc edge under the assumptions of constant tangential velocity and constant film thickness. At first, the liquid film will be considered inviscid and of large depth and later the effects of viscosity will be included.

2.0 INVISCID SOLUTION

With reference to Figure 4, we let $y = 0$ correspond to the undisturbed free surface and perturb the surface an infinitesimal amount η. We constrain $-h < y < h'$ where h is the film thickness. Later, we will let $h' \to \infty$, since the air is assumed to be unbounded around the rotating disc.

Let the liquid have tangential velocity V_T and density ρ, and let the air have corresponding parameters V'_T and ρ'. The surface tension of the liquid is T. The perturbation potentials ϕ_1 of the liquid and ϕ'_1 of the air must satisfy Laplace's equation,

and the pressure must satisfy a surface condition to be discussed later at y = 0. In addition, the velocities normal to the free surface of liquid, air and the surface itself must be compatible. No flow is allowed when y = -h or h' since the disc is solid (y=-h) and the disturbance potential of the air (ϕ'_1) must be zero at the boundary of the air (y=h').

2.1 Disturbance Velocity Potential

To satisfy the above requirements, we assume the following forms for the disturbance potentials ϕ_1 and ϕ'_1 (Lamb[2]):

$$\phi_1 = C \cosh [k(y+h)] \; e^{i(\sigma t - kr\theta)} \tag{1}$$

$$\phi'_1 = C' \cosh [k(y-h')] \; e^{i(\sigma t - kr\theta)} \tag{2}$$

where $k = 2\pi/\lambda$ and λ is the wavelength of the disturbance. These forms satisfy Laplace's equation ($\nabla^2\phi_1 = 0$, $\nabla^2\phi'_1 = 0$), and the velocity conditions ($\partial\phi_1/\partial y = 0$ at $y = -h$, $\partial\phi'_1/\partial y = 0$ at $y = h'$).

2.2 Pressure Condition at the Free Surface

Surface tension forces allow a curved surface to support a pressure drop according to the law

$$P - P' = T \left(\frac{1}{R_1} + \frac{1}{R_2}\right)$$

where R_1 and R_2 are the free surface radii of curvature in the r,θ plane and axial directions respectively (Lamb[2] p. 471). Now, $1/R_1 = 1/r' - (d^2r'/d\theta^2)/r^2$ where r' is the perturbed free surface shape. Here, $r' = r+\eta$ and η is the surface perturbation relative to y = 0. From Lamb,

$$P - P' = T \left(\frac{1}{(r+\eta)} - \frac{1}{(r+\eta)^2} \frac{\partial^2(r+\eta)}{\partial\theta^2} - \frac{\partial^2(r+\eta)}{\partial z^2}\right) \tag{3}$$

In Equation 11 we will neglect variation of η with z; i.e., in the direction of the spin axis ($R_2 = \infty$). Expanding Equation 3 and retaining only first order quantities of η and its derivatives results in

$$P - P' = \frac{T}{r} - \frac{T}{r^2}\left(\eta + \frac{\partial^2\eta}{\partial\theta^2}\right)$$

We assume that $\eta << \partial^2\eta/\partial\theta^2$. This term could be retained but little accuracy is gained when the angular velocity is large. The perturbation terms p and p' are hence related by the perturbation equation

$$p - p' + \frac{T}{r^2}\frac{\partial^2\eta}{\partial\theta^2} = 0 \tag{4}$$

2.3 Surface Conditions for Velocity

The conditions that the normal velocity of the fluids be the same as that of the free surface for small deflections and that the tangential velocity is the only significant velocity component leads to:

$$\frac{\partial\eta}{\partial t} + \frac{V_r}{r}\frac{\partial\eta}{\partial\theta} = -\frac{\partial\phi_1}{\partial y} \tag{5}$$

$$\frac{\partial \eta}{\partial t} + \frac{V'_r}{r}\frac{\partial \eta}{\partial \theta} = -\frac{\partial \phi'_1}{\partial y} \qquad (6)$$

2.4 The Equations of Motion

The perturbation quantities must satisfy linearized forms of the equation of motion (Lamb[2])

$$\frac{P_s + p}{\rho} = \frac{\partial \phi_1}{\partial t} - \tfrac{1}{2}\left[\left(V_r - \frac{1}{r}\frac{\partial \phi_1}{\partial \theta}\right)^2 + \left(\frac{\partial \phi_1}{\partial y}\right)^2\right] - (-r\Omega^2 \sin\alpha + g\cos\alpha)\eta \qquad (7)$$

$$\frac{P'_s + p'}{\rho'} = \frac{\partial \phi'_1}{\partial t} - \tfrac{1}{2}\left[\left(V'_r - \frac{1}{r}\frac{\partial \phi'_1}{\partial \theta}\right)^2 + \left(\frac{\partial \phi'_1}{\partial y}\right)^2\right] - (-r\Omega^2 \sin\alpha + g\cos\alpha)\eta \qquad (8)$$

where p and p' are perturbation pressures relative to the steady pressures P_s and P'_s. The centrifugal force modifies the usual force potential in the last term of Equations 7 and 8. When Ω is large, it is reasonable to neglect g with respect to $r\Omega^2$. In any event, the angle α is nearly 90°. Expanding Equations 7 and 8, neglecting steady terms and linearizing we get the following perturbation equations:

$$p/\rho = \frac{\partial \phi_1}{\partial t} + \frac{V_r}{r}\frac{\partial \phi_1}{\partial \theta} + r\Omega^2\eta \qquad (9)$$

$$p'/\rho' = \frac{\partial \phi'_1}{\partial t} + \frac{V'_r}{r}\frac{\partial \phi'_1}{\partial \theta} + r\Omega^2\eta \qquad (10)$$

Under the assumptions, $\sin\alpha$ is taken to be one.

2.5 Surface Shape

We assume that the perturbation to the surface elevation can be written

$$\eta = ae^{i(\sigma t - kr\theta)} \qquad (11)$$

Note that $\partial^2\eta/\partial\theta^2$ is $(kr)^2\eta$ justifying the approximation in Equation 4 for large k.

2.6 Development of Stability Criteria

We substitute Equations 1 and 11 in Equation 9 and obtain

$$p/\rho = \left[C \cosh\left\{k(y+h)\right\}\left\{i(\sigma - kV_r)\right\} + r\Omega^2 a\right]e^{i(\sigma t - kr\theta)} \qquad (12)$$

Similarly, Equations 2 and 11 substituted into Equation 10 yields

$$p'/\rho' = \left[C' \cosh\left\{k(y-h')\right\}\left\{i(\sigma - kV'_r)\right\} + r\Omega^2 a\right]e^{i(\sigma t - kr\theta)} \qquad (13)$$

We apply the pressure condition, substitute Equations 12 and 13 into Equation 4, set $y = 0$, retain only perturbations and simplify. The result is:

$$\rho C \cosh kh(i)(\sigma - kV_T) - \rho' C' \cosh kh'(i)(\sigma - kV'_T) = a\left[Tk^2 - (\rho - \rho')\, r\Omega^2\right] \tag{14}$$

The surface conditions (Eqs. 5 and 6) yield:

$$C = - ai(\sigma - kV_T)/(k \sinh kh) \tag{15}$$

$$C' = + ai(\sigma - kV'_T)/(k \sinh kh') \tag{16}$$

Substituting Equations 15 and 16 in Equation 14 results in:

$$\rho \coth kh\left(\frac{\sigma}{k} - V_T\right)^2 + \rho' \coth kh'\left(\frac{\sigma}{k} - V'_T\right)^2 = Tk - (\rho - \rho')\, r\Omega^2/k \tag{17}$$

We solve for (σ/k) in Equation 17 and let $S = \rho' \coth kh'/\rho \coth kh$ and get

$$\left(\frac{\sigma}{k}\right) = \frac{V_T + SV'_T}{1 + S} \pm \frac{\sqrt{S}}{1 + S} \sqrt{-(V_T - V'_T)^2 - (1+S)(\rho/\rho')\left[\frac{r\Omega^2}{k}(1 - \rho'/\rho) - \frac{Tk}{\rho}\right]} \tag{18}$$

The wave speed is σ/k.

Examination of Equation 18 shows that σ will be complex $(\gamma \pm i\delta)$ if the quantity f(k) under the root sign is negative. From Equation 18,

$$f(k) = - (V_T - V'_T)^2 - (1+S)(\rho/\rho')\left[\frac{r\Omega^2}{k}(1 - \rho'/\rho) - \frac{Tk}{\rho}\right] \tag{19}$$

If f(k) is negative, then the perturbation amplitude η becomes

$$\eta = ae^{i(\gamma t + \ell k)}\, e^{\pm \delta t}$$

which is divergent. Hence, if f(k) from Equation 19 is less than zero, the wave is unstable. Setting f(k) equal to zero defines a boundary for stability. In the present application, the relative velocity between the liquid and the stationary air $(V_T - V'_T)$ is just $r\Omega$. Further, $h' \simeq \infty$ and the factor S reduces to (ρ'/ρ) tanh kh which is $<<1$. The density ratio ρ'/ρ is also very small for air-liquid combinations. Hence, we approximate Equation 19 by

$$f(k) \simeq - (r\Omega)^2 - (\rho/\rho')\left[\frac{r\Omega^2}{k} - \frac{Tk}{\rho}\right] \leq 0 \tag{20}$$

and obtain an approximate stability criterion. Equation 20 is quadratic in k. We define

$$\lambda^* = \frac{\lambda}{2\pi r} = (kr)^{-1} \tag{21}$$

as a nondimensional disturbance wavelength. Substitution of Equation 21 in Equation 20

leads to the following expression for $f(\lambda^*)$:

$$f(\lambda^*) = \lambda^{*2} + (\rho'/\rho)\lambda^* - 1/W \geq 0 \tag{22}$$

where W is Weber's Number defined by

$$W = \frac{rV_r^2\rho}{T} \tag{23}$$

There is one real positive root to Equation 22 denoted by λ^*_1. Figure 5 illustrates the range of λ^* for stable or unstable waves.

Solving Equation 22 for λ^*_1 leads to the following limit on λ^* for unstable surface waves:

$$\lambda^* > \lambda^*_1$$

$$\lambda^*_1 = \frac{\rho'/\rho}{2}\left[-1 + \sqrt{1 + \frac{4}{(\rho'/\rho)^2 W}}\right] \tag{24}$$

If $\lambda^*_1 < \lambda^*$ an unstable surface wave results.

Pedley[3] neglected the air inertia ($\rho' = 0$) in his analysis but he did not make the assumption $\eta << \frac{\partial^2\eta}{\partial\theta^2}$ (Eq. 4). He quotes the result of Hocking[4] for the necessary and sufficient conditions for stability as

$$W < \frac{1}{\lambda^*}\left(\frac{1}{\lambda^*} + 1\right)$$

$$< \frac{1}{\lambda^{*2}} \text{ when } \eta << \frac{\partial^2\eta}{\partial\theta^2} \tag{25}$$

where the notation has been made to agree with this work. Setting $\rho' = 0$ in Equation 22 leads to $\lambda^{*2} \geq 1/W$ for instability, which is the same as Hocking's result. Since the maximum value of λ^* is one, and since there must be an integral number of wavelengths in order for a periodic surface wave to exist, it is easily seen that $\sqrt{W} = 1, 2, 3, \ldots . n$ for this special case. More generally, we can include the air inertia ($\rho' \neq 0$) and obtain from Equation 22

$$W \geq \frac{n^2}{1 + (\rho'/\rho)n} \qquad n = 1, 2, \ldots . \tag{26}$$

for instability. Properly, $n > 10$ for the approximation $\eta << \frac{\partial^2\eta}{\partial\theta^2}$. Now ρ'/ρ is of order 10^{-3} for air-liquid interfaces, so that for $n < 10^2$, $W \geq n^2$ is a good approximation to the instability criterion while for $n \geq 10^4$, $W \geq \frac{n\rho}{\rho'}$ is better. For W sufficiently high, a wide range of disturbance wavelengths lead to an unstable free surface. Squire[5] has shown that a sheet of liquid moving in still air is unstable provided the Weber Number (based on one half the sheet thickness) is greater than one. He quotes fair agreement with experiment.

2.7 Effect of Parameters on Surface Stability

The surface tension enters the problem only in the Weber Number W. As $T \rightarrow 0$, $W \rightarrow \infty$ and the stability criterion of Equation 22 reduces to

$$f(\lambda^*) = \lambda^*(\lambda^* + \rho'/\rho) > 0 \tag{27}$$

This is satisfied by all positive λ^* and shows the stabilizing effect of surface tension in the sense that a smaller range of values of λ^* result when $T \neq 0$.

The result of Equation 27 is reproduced by large values of r or Ω. For a given disc, the higher the angular velocity the wider the range of λ^* for unstable waves. Hence, Ω is a "destabilizing" variable.

The density ratio ρ'/ρ can vary by choice of liquid (ρ) and its temperature as well as by varying ambient conditions of air temperature and pressure (ρ'). The addition of ρ'/ρ acts in a destabilizing sense. Increasing ρ acts in a stabilizing sense while the converse is true for ρ'.

2.8 Maximum Instability with "Large" Film Thickness

Some disturbance wavelength in the unstable region maximizes the imaginary part of σ, leading to a "fastest growing" disturbance. From Equations 18 and 21 we obtain the following expression for σ:

$$\sigma = \frac{V_r}{\lambda^* r} \pm \frac{i}{r\lambda^*} \sqrt{\rho'/\rho \tanh kh} \sqrt{g(\lambda^*)} \tag{28}$$

where

$$g(\lambda^*) = + V_r^2 + (\rho/\rho')V_r^2\lambda^* - (\rho/\rho') \frac{T}{r\rho} \frac{1}{\lambda^*} \tag{29}$$

The hyperbolic tangent is nearly 1 when kh is greater than about 1.5. In this sense, we let kh be "large", and let tanh kh = 1 in Equation 28. The result for the imaginary part of σ is:

$$\mathrm{Im}(\sigma) = \frac{1}{r} \sqrt{\rho'/\rho} \sqrt{\frac{g(\lambda^*)}{\lambda^{*2}}} \tag{30}$$

The condition for maximum instability is:

$$\frac{d[\mathrm{Im}(\sigma)]}{d\lambda^*} = 0 \tag{31}$$

or

$$\frac{d}{d\lambda^*} \left[\frac{g(\lambda^*)}{\lambda^{*2}}\right] = 0 \tag{32}$$

The operation indicated by Equation 32 is applied to Equation 29 which results in:

$$\lambda^{*2} + 2(\rho'/\rho)\lambda^* - \frac{3}{W} = 0 \tag{33}$$

for finite λ^*.

Equation 33 is quadratic in λ^* and it has one root (λ^*_{CRIT}) within the unstable region:

$$\lambda^*_{CRIT} = (\rho'/\rho)\left[-1 + \sqrt{1 + \frac{3}{(\rho'/\rho)^2 W}}\right] \tag{34}$$

Disturbances with wavelength equal to λ^*_{CRIT} are those which grow the fastest. Substituting Equation 34 in Equation 28 leads to the corresponding complex value of σ. Note that $1/\lambda^*_{CRIT}$ must be an integer leading to the conclusion that very often there is no physically possible solution to Equation 34. Hence any λ^* in the unstable range is equally likely. The higher the Weber Number, the more likely a solution to Equation 34 becomes.

Integral values of $(\lambda^*)^{-1}$ and $(\lambda^*_{CRIT})^{-1}$ were chosen and the corresponding Weber Number for $\rho = 1.65$ slugs/ft^3 and $T/\rho = .0015$ ft^3/sec^2 was computed from Equations 24 and 33. The results are shown in Figure 6. Properly, the points should not be joined by a smooth curve.

For many liquids, T/ρ does not vary outside the range 0.5×10^{-3} to 2.5×10^{-3}. Below a certain speed, the waves are stable. For example, for $(\lambda^*_1)^{-1} = 10$, the waves are stable for $r^3\Omega^2 < .148$, $(T/\rho = .0015)$. The smaller the radius, the higher this minimum speed becomes. It is seen that λ^*_{CRIT} is close to λ^*_1. For $W < 10^5$, $\log (\lambda^*_1)^{-1}$ is approximately a linear function of $\log W$ with a slope of .52. Hence, for inviscid fluids, $(\lambda^*_1)^{-1} = W^{.52} + \text{constant}$.

3.0 VISCOUS SOLUTION FOR "LARGE" DEPTH

Lamb[2] (p. 627) considers surface waves of a stationary viscous fluid. He concludes that the wave velocity is very nearly the same as for an inviscid solution but that the amplitude of the wave is attenuated approximately by a factor $e^{-2\nu k^2 t}$. The parameter ν is the kinematic viscosity of the liquid. Harrison[4] has analyzed the viscous problem more accurately and we interpret Lamb's result as applying when $\rho'\nu' << \rho\nu$. The restriction is easily met for air-liquid interfaces even if $\nu' > \nu$. Further, the flow irrotationality assumption becomes more approximate the nearer one gets to the disc surface since viscous forces increase as $y \to -h$. Therefore, we add a further condition that the results will be accurate only when $h > \frac{1}{2}\lambda$. In this event, the factor S from Equation 18 is just ρ'/ρ, and we restrict ourselves to large depth solutions.

With the above comments in mind, we replace Equation 11 by

$$\eta = ae^{-2\nu k^2 t} e^{i(\sigma t - kr\theta)} \tag{35}$$

and retain the wave velocity σ/k from Equation 18. A slight revision of the instability criterion is necessary. As before, let $\sigma = \gamma \pm i\delta$ and substitute it into Equation 35 and obtain

$$\eta = ae^{(-2\nu k^2 \pm \delta)t} e^{i(\gamma t - kr\theta)} \tag{36}$$

From Equation 36, η will be divergent if

$$m(k) = -2\nu k^2 + \delta > 0 \tag{37}$$

Using Equation 28 to evaluate δ, we have

$$-2\nu k^2 + k\sqrt{\rho'/\rho}\,\sqrt{g(k)} \geq 0 \tag{38}$$

for an instability criterion where g(k) is given by Equation 29. As before, we substitute

$\lambda^* = (kr)^{-1}$ and solve for λ^*:

$$h(\lambda^*) = \lambda^{*3} + (\rho'/\rho)\lambda^{*2} - (1/W)\lambda^* - 4/Re^2 \geq 0 \qquad (39)$$

One positive real root of Equation 39 always exists and defines a stability boundary. Two negative real roots always exist. Figure 7 shows the stability boundary as a function of Reynolds Number for various values of Weber Number. Values of ρ' and ρ are the same as those for Figure 6.

All the curves coalesce at low Reynold's Number which shows that the stability boundary for very viscous fluids is insensitive to surface tension.

Each stability boundary in Figure 7 tends to rise linearly and then roll off to the inviscid assymptote as Reynold's Number increases. The roll-off point is a function of Weber Number. The linear portion can be approximated by

$$(\lambda_1^*)^{-1} = Re^{.7} + C$$

When viscosity is zero ($Re \to \infty$) then Equation 39 yields the same roots as its inviscid counterpart Equation 23. The addition of viscosity results in a smaller region of unstable wavelengths and hence is said to exert a "stabilizing" influence on the free surface.

The wave velocity of the unstable viscous fluid is identical with the inviscid and equals the tangential velocity V_T. The wave is stationary with respect to the disc.

3.1 Effect of Flow Rate

For a given fluid, disc and speed, the value of $\bar{h}$ depends only on the flow rate. An approximate equation for $\bar{h}$[11] is:

$$\bar{h} = \frac{1}{r}\sqrt{\frac{\nu}{\Omega}}\left(\frac{3Q}{2\pi r^2\sqrt{\Omega\nu}\,\dot{r}}\right)^{1/3}$$

After some manipulation, the most useful form for $\bar{h}$ is:

$$\bar{h} = \left(\frac{(6\pi)Q}{a^{*2}ReV_T\dot{r}}\right)^{1/3}$$

where a^* is the circumference of the rotating body and $\dot{r}$ is the local slope. It is seen that $\bar{h}$ varies as $Q^{1/3}$.

As $\alpha \to \pi/2$ $\dot{r} \to 0$ leading to a large film thickness but $\bar{h}$ is nearly constant for a range which ends quite close to $\alpha = \pi/2$. It is easily seen that a very small film thickness can result from high values of V_T and Re or low values of Q. Hence, small values of λ^* are physically possible that are well within the limitations that $\lambda < 2h$.

3.2 Atomization and Instability

The above theory on surface instability is applied in the formulation of a new theory on the mechanism of atomization from rotating bodies. Consider the sketch in Figure 8. When $\lambda^* > \lambda_1^*$, the free surface is unstable, η tends to h as time progresses and a volume of liquid equal to $\lambda^2 h$ is trapped in the shaded area. Since η is periodic in θ (period = λ^*), the number of "sites" of formation is constant around the body, and the amount of flow to any site is $\lambda^* Q$ ft^3/sec. Macfarlane and Colbourn[11] have verified this experimentally.

Using Equations 18 and 35, we can write

$$\eta = e^{n(\lambda^*)t} \; e^{\frac{i(\Omega t - \theta)}{\lambda^*}} \tag{40}$$

$$\dot{\eta} \cong \left(n + i \frac{\Omega}{\lambda^*}\right) \eta \tag{41}$$

If n is large, then the perturbation grows rapidly. The phase shift between η and $\dot{\eta}$ is about 90° because Ω and n are large while λ^* is small. The result is a large outward velocity over the rising portion of the wave and a corresponding large inward velocity over the falling portion of the wave. Hence, the trapped volume will leave the rotating body normal to the free surface with a considerable amount of internal rotation. Three types of atomization have been experimentally observed[6,7] from rotating discs and cups:

1) direct drop formation at low Q,
2) ligament formation at moderate Q,
3) sheet formation at high Q.

Ligaments decay into drops by Rayleigh-type surface instability of rotationally symmetric columns of fluids, while sheets decay into ligaments by a surface instability (Hagerty and Shea[8] or Dombrowski and Johns[9]) and subsequently into drops by Rayleigh instability. The flow rate Q determines which type of atomization results. Now, if $\lambda^2 h$, the volume of trapped fluid, is greater than $\lambda^* Q \Delta t$, the flow to the site, then type 1 atomization results in an intermittent manner because it takes a finite time to replenish the fluid and rebuild the fluid layer for a subsequent unstable ejection of fluid. However, if $\lambda^2 h$ is about equal to $\lambda^* Q \Delta t$, then continuous ejection of ligaments must occur in order to satisfy the continuous flow. Obviously, the third condition of sheet ejection results when $\lambda^* Q \Delta t$ is greater than $\lambda^2 h$. Probably Δt will have to be studied experimentally, but it probably is related to $n(\lambda^*)$ (Eq. 40).

If the instability criterion is not met, then the linear approximation predicts a stable flow which separates as a sheet from the rotating body independent of the flow rate. If the flow rate is low, then the film is very thin resulting in a very short sheet which very quickly decays to drops.

Historically, the accepted mechanism of drop formation from the edge of a disc has been to equate the mass of the drop times its centripetal acceleration with the surface tension force based on the drop circumference. The correlation function due to Walton and Prewett[10] is

$$d\Omega \sqrt{\frac{\rho r}{T}} = \text{constant} \tag{42}$$

$$d\Omega \sqrt{\frac{\rho r}{T}} = \text{constant} \tag{42}$$

where d is the drop diameter. The constant in Equation 42 did not correlate well using experimental values of parameters on the lefthand side.

The only steady surface tension effects are the rise of fluid in a capillary tube and the ability of the curved free surface to support a steady pressure difference. The former requires fluid contact on both sides of a tube normal to the free surface while the latter is subtracted out exactly from the perturbation equations. Therefore, surface tension forces arise only from altering the curvature of the steady free surface due to free-surface perturbations. Only when the surface is "stretched" should surface forces be considered. Hence it is unsatisfying to equate surface tension forces whose origin is in unsteady phenomena with centripetal accelerations which are steady when Ω is constant.

Rayleigh instability of fluid ligaments arises from a surface instability and now a consistent drop formation process from rotating discs based on surface instability is proposed. Hinze and Milborn[7] applied an instability approach in attempting to explain and correlate their experimental results. However, their point of view was qualitative and was used only to collect variables in functional groups for experimental determination of a constant and an exponent. Pedley[3] hints at surface instability being involved in atomization of swirling liquid jets.

As the amplitude of the surface wave increases, the linearized form of the equations presented here becomes less accurate and the λ^* of the actual wave may differ from the theoretically predicted value. However, if a non-linear system is unstable to an infinitesimal disturbance, so is its linearized approximation. Hence, the extension of the proposed drop formation process to real situations is immediate.

3.3 Comparison of Theory with Available Experimental Data

Experimental work which supplies sufficient data to calculate λ_1^* is sparse. Either the fluid or the operating conditions are not completely documented. However, an exception is the paper by Hinze and Milborn[7], although even their method of presentation leaves doubt as to the values of all the parameters for any specific data point. Their main contribution to the present comparison is a semi-empirical relation for the number of ligaments shed from a rotating cup. They present the relation

$$z = K\left(\frac{\rho\Omega^2 D^3}{T}\right)^{\frac{2}{4+n}}\left(\frac{\rho T D}{\mu^2}\right)^{\frac{n}{4+n}} \tag{43}$$

for the number of ligaments. K and n were found to be .215 and 4/5 from experiment. A reasonably large amount of scatter (±25%) existed. In the notation of this paper and noting z aquals $1/\lambda^*$ we get (from Eq. 43):

$$\lambda^* = 1/(.577\mathrm{Re}^{1/3}\mathrm{W}^{1/4}) \tag{44}$$

In arriving at this equation, Hinze and Milborn allowed Q to vary provided that the flow rate was not high enough to produce a sheet and yet high enough to exclude direct drop formation. In addition, data for three different liquids were presented.

They noted a "liquid torus" formed at the lip of the cup. This is a reasonable situation since the steady radial velocity of the liquid varies from zero on the cup surface to a maximum at the free surface and the inward directed normal velocity has the same behaviour resulting in a tendency for the liquid to flow around the edge of the cup lip. Hence, the approximation of α in the stability equations being equal to 90° is appropriate.

The results of the stability analysis using parameter values within the experimental range are compared with the experimental results of the three liquids as well as the overall correlation function (Eq. 44) on Figures 9 to 11. The viscosity of the liquids was the major variation between them.

On Figure 9, the experimental data for the least viscous liquid virtually coincided with the viscous stability boundary, as did the overall correlation function. The comparison is very good. Increasing viscosity (Fig. 10) showed the overall correlation function close to the viscous stability boundary but the particular liquid curve showed some discrepancy. The highest viscosity liquid (Fig. 11) was within the stable region as predicted by the viscous boundary, but was within the unstable region from the inviscid boundary. Apparently non-linear and rotational flow effects have become important. In general, the comparison is favourable considering the comments on scatter and variable

Q already made. This tends to substantiate the theory of this report. When the theory predicts instability, Hinze and Milborn's data show ligaments. The only area where discrepancies occur is for very viscous liquids.

A further check on experimental results was made from a photograph by Macfarlane and Colbourn[11] showing atomization by direct drop formation from the edge of a spinning disc. The picture was a shadowgraph taken looking vertically down on a 13.4° sector of a one-inch diameter disc. The regularity of drop formation sites was evident and 23 were counted at the rim of the sector. The angular velocity was 313 revolutions per second. Regarding each drop site as a wavelength, it was easy to calculate $\lambda^* = 3.2 \times 10^{-3}$. The fluid data were not specified but by using T/ρ of 1.2×10^{-3}, ρ'/ρ of 1.4×10^{-3}, and $\nu = 10^{-4}$ (the fluid was a light fuel oil) the inviscid and viscous boundary calculations for λ_1^* were 1.5×10^{-3} and 2.2×10^{-3} respectively. Therefore, the theory did predict an unstable surface wave and the proposed atomization model was not contradicted.

However, Stuart[12], in his review article on non-linear effects in hydrodynamic stability, points out that Poisseuille Flow can be unstable due to non-linear effects when the flow is predicted to be stable by linearized theory. There may be an energy transfer from the perturbed motion to the mean motion by Reynold's Stresses which distort the mean flow. Rosenhead[13] states that non-linear terms do not act to stabilize a flow and that plane Couette Flow is unstable for finite disturbances even though it is stable for infinitesimal disturbances. The linear theory is thus considered to be somewhat restrictive since it does not account for any energy transfers between the mean and perturbed motions.

Lamb[2] (p. 417) discusses waves of finite amplitude. The free surface of a quiescent liquid of infinite depth takes on an "approximately trochoidal form" which sharpens the crests and flattens the troughs of the sine wave predicted by linear theory. This is exactly what the pictures of Hinze and Milborn show for ligament formation, i.e. the space between the ligaments is greater than a ligament diameter.

The linearized theory is valid only when a/λ is small (Lamb[2] p. 417). In other words, the amplitude of the surface wave must be much less than its wavelength. For irrotationality, h must be greater than $\lambda/2$. Therefore, the wave amplitude is restricted to being much less than h. For atomization, the amplitude must equal the film thickness which leads to the conclusion that the linearized theory can only be used to test for incipient instability.

4.0 CONCLUSION

A surface-wave instability theory has been presented to attempt an explanation of drop and ligament formation from edges of rotating discs and cups. Sheet formation has already been explained by the separation of the fluid from the edge of the rotating disc by the steady flow theory (Drummond[1]). Pedley's[3] results have been extended. Some correlation between theory and experimental results of Hinze and Milborn[7] and Macfarlane and Colbourn[11] have been shown which tends to substantiate the theory. However, the linear theory may be too restrictive and non-linear as well as rotational flow effects may be large during the actual fluid shedding from the disc edge.

Atomization from sheets and isolated ligaments has already been explained by free-surface instability, and now atomization from rotating cups and discs has been put in the same framework. Some experimental work is needed to provide data on edge waves and their breakdown.

5.0 REFERENCES

1. Drummond, A.M. — Steady Viscous Flow With a Free Surface On a Rotating Axisymmetric Body. Assoc. Committee on Agricultural and Forestry Aviation, National Research Council of Canada, AFA-TN-10, 1972.

2. Lamb, H. — Hydrodynamics, Sixth Edition, Cambridge University Press, 1932.

3. Pedley, T. J. — The Stability of Rotating Flows with a Cylindrical Free Surface. Journal of Fluid Mechanics, Vol. 30, Part 1, 1967, pp. 127-147.

4. Hocking, L. M. — Mathematika, Vol. 7, No. 1.

5. Squire, H. B. — Investigation of the Instability of a Moving Liquid Film. British Journal of Applied Physics, Vol. 4, June 1953, pp. 167-169.

6. Fraser, R. P. Dombrowski, N. Routley, J. H. — The Filming of Liquids by Spinning Cups. Chem. Eng. Sci., Vol. 18, 1963, pp. 323-337.

7. Hinze, J. O. Milborn, H. — Atomization of Liquids by Means of a Rotating Cup. Journal of Applied Mechanics, Vol. 17, No. 2, June 1950, pp. 145-153.

8. Hagerty, W. W. Shea, J. F. — A Study of the Stability of Plane Fluid Sheets. Journal of Applied Mechanics, Vol. 22, No. 4, December 1955, pp. 509-514.

9. Dombrowski, N. Johns, W. R. — The Aerodynamic Instability and Disintegration of Viscous Liquid Sheets. Chem. Eng. Sci., Vol. 18, 1963, pp. 203-214.

10. Walton, W. H. Prewett, W. C. — The Production of Sprays and Mists of Uniform Drops Size by Means of Spinning Disc Type Sprayers. Proc. Physical Society, Section B, Vol. 62, Part 6, No. 354B, June 1949, pp. 341-350.

11. Macfarlane, J. J. Colbourn, A. J. — A Study of the Performance of Rotary Atomisers. NGTE R-310, July 1969.

12. Stuart, J. T. — Non-Linear Effects in Hydrodynamic Stability. Proc. of the Tenth Int. Cong. of Applied Mechanics, Stresa, 1960, Elsevier Publishing Co., 1962, pp. 63-97.

13. Rosenhead, L. — Laminar Boundary Layers. Fluid Motion Memoirs, Oxford University Press, 1963.

14. Harrison, W. J. — The Influence of Viscosity on the Oscillations of Superposed Fluids. The London Mathematical Society, Second Series, Vol. 6, April 1908, pp. 396-405.

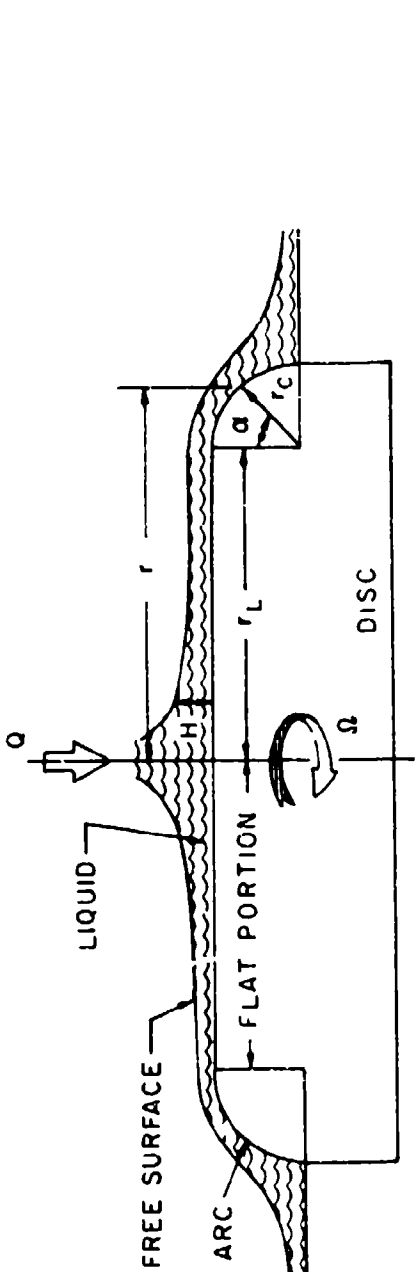

FIG. 1 : SCHEMATIC OF ROTATING DISC

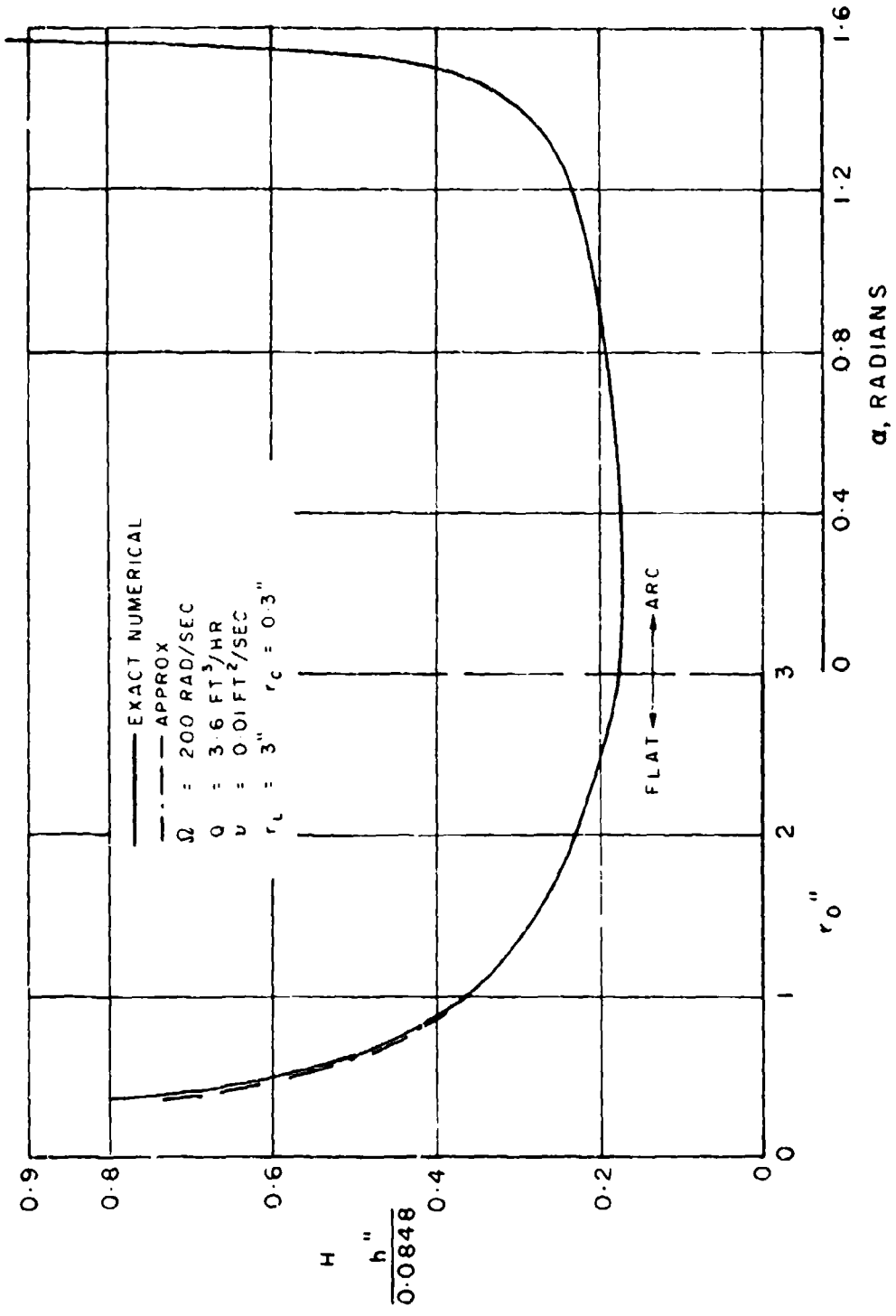

FIG.2: REPRESENTATIVE FILM THICKNESS ON THE FLAT PORTION AND CIRCULAR ARC EDGE OF A SPINNING DISC (REF 1)

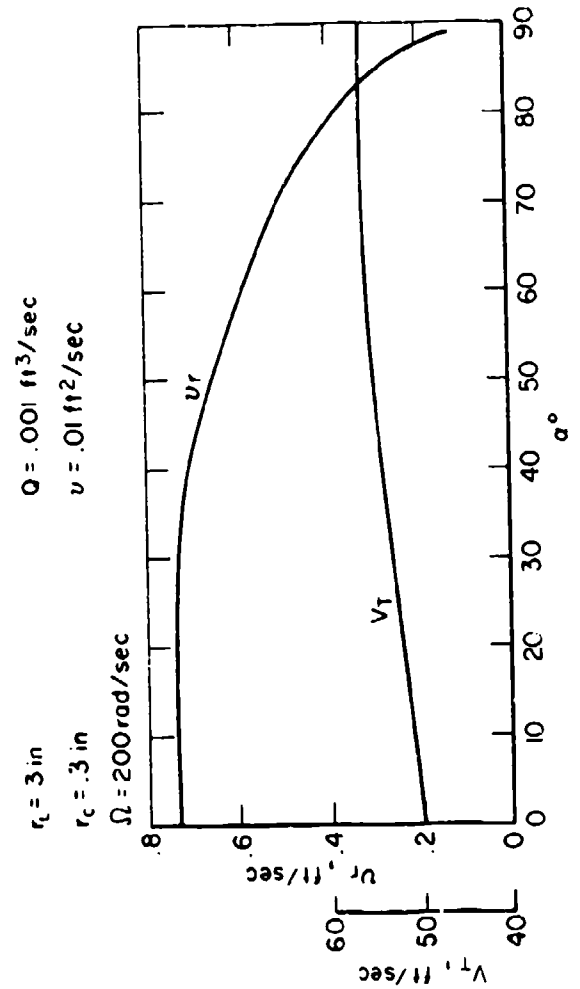

FIG. 3: REPRESENTATIVE RADIAL AND TANGENTIAL VELOCITIES AT THE FREE SURFACE ON THE CIRCULAR ARC EDGE OF A ROTATING DISC (REF 1)

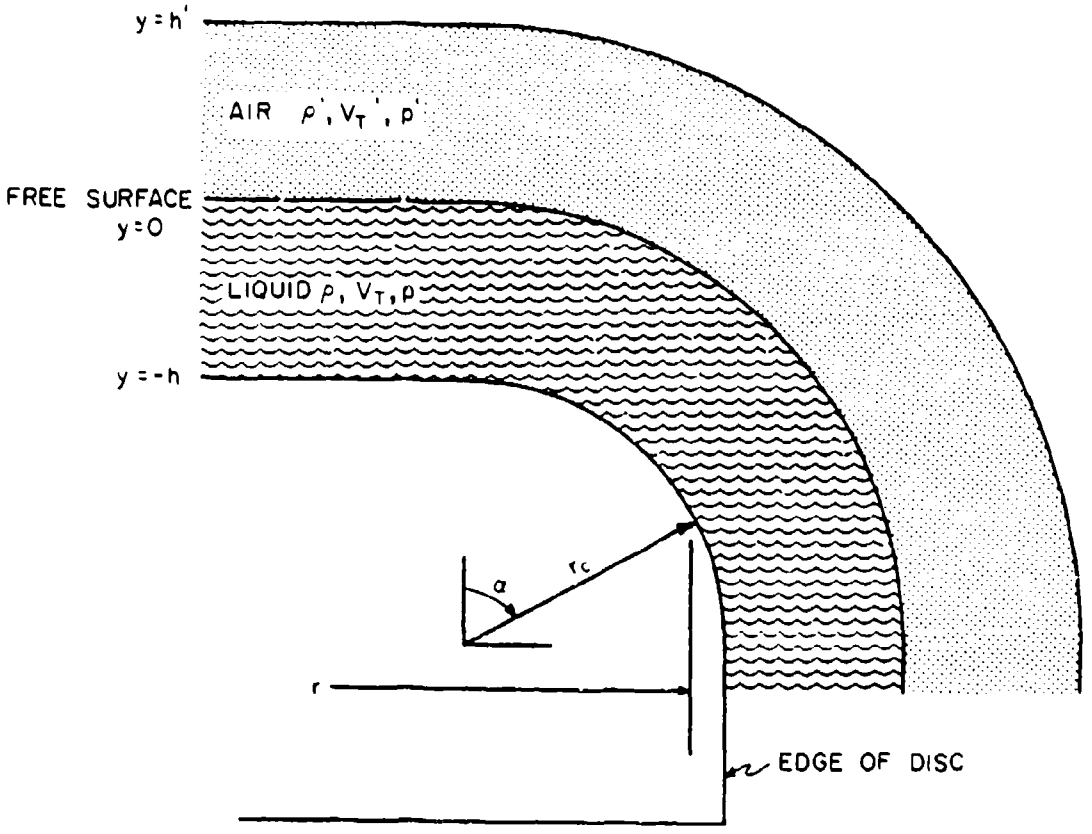

FIG. 4: SCHEMATIC OF EDGE FLOW ON A ROTATING DISC

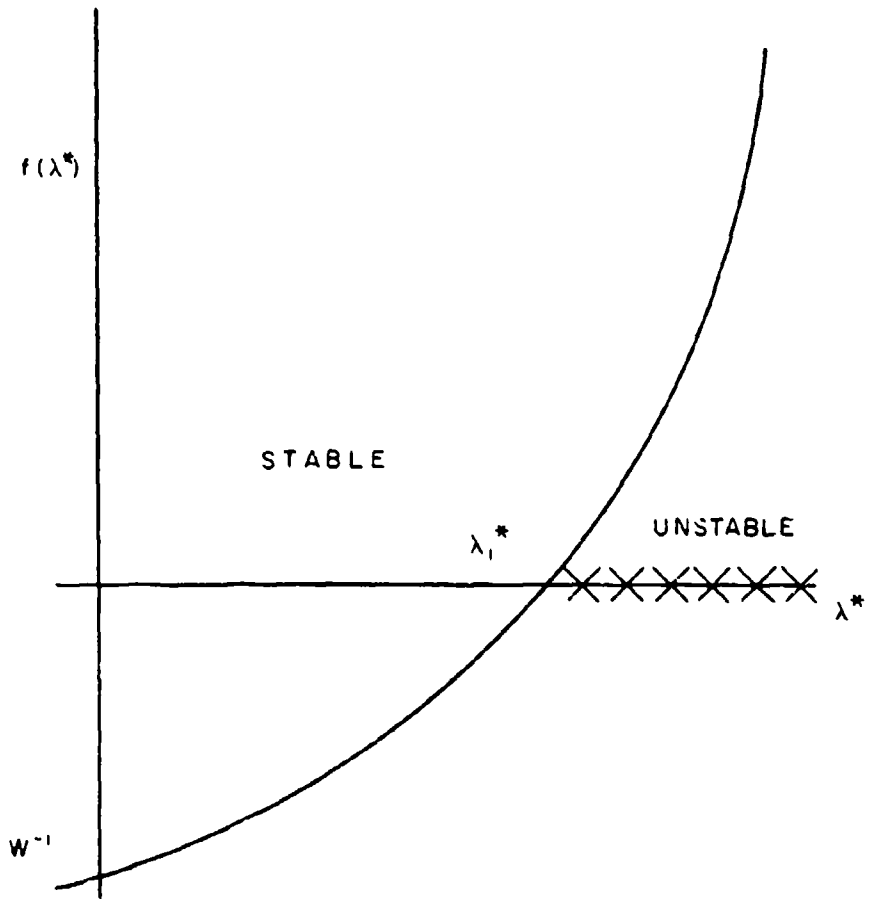

FIG. 5: SCHEMATIC OF THE STABILITY CRITERION FOR INVISCID FLOW

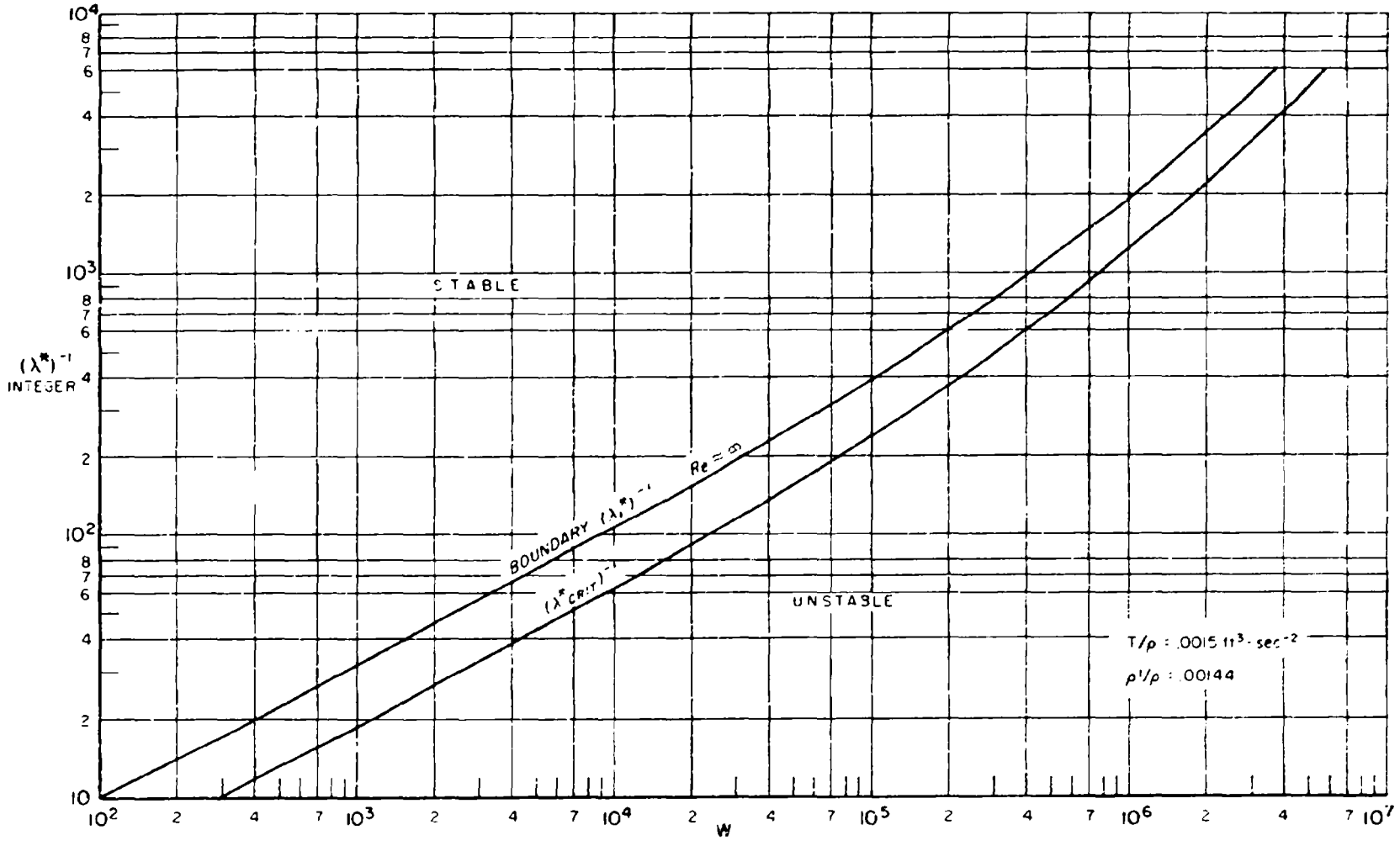

FIG. 6: STABILITY BOUNDARY AND FASTEST GROWING WAVE AS A FUNCTION OF WEBER NUMBER FOR INVISCID FLOW AND LARGE FILM THICKNESS

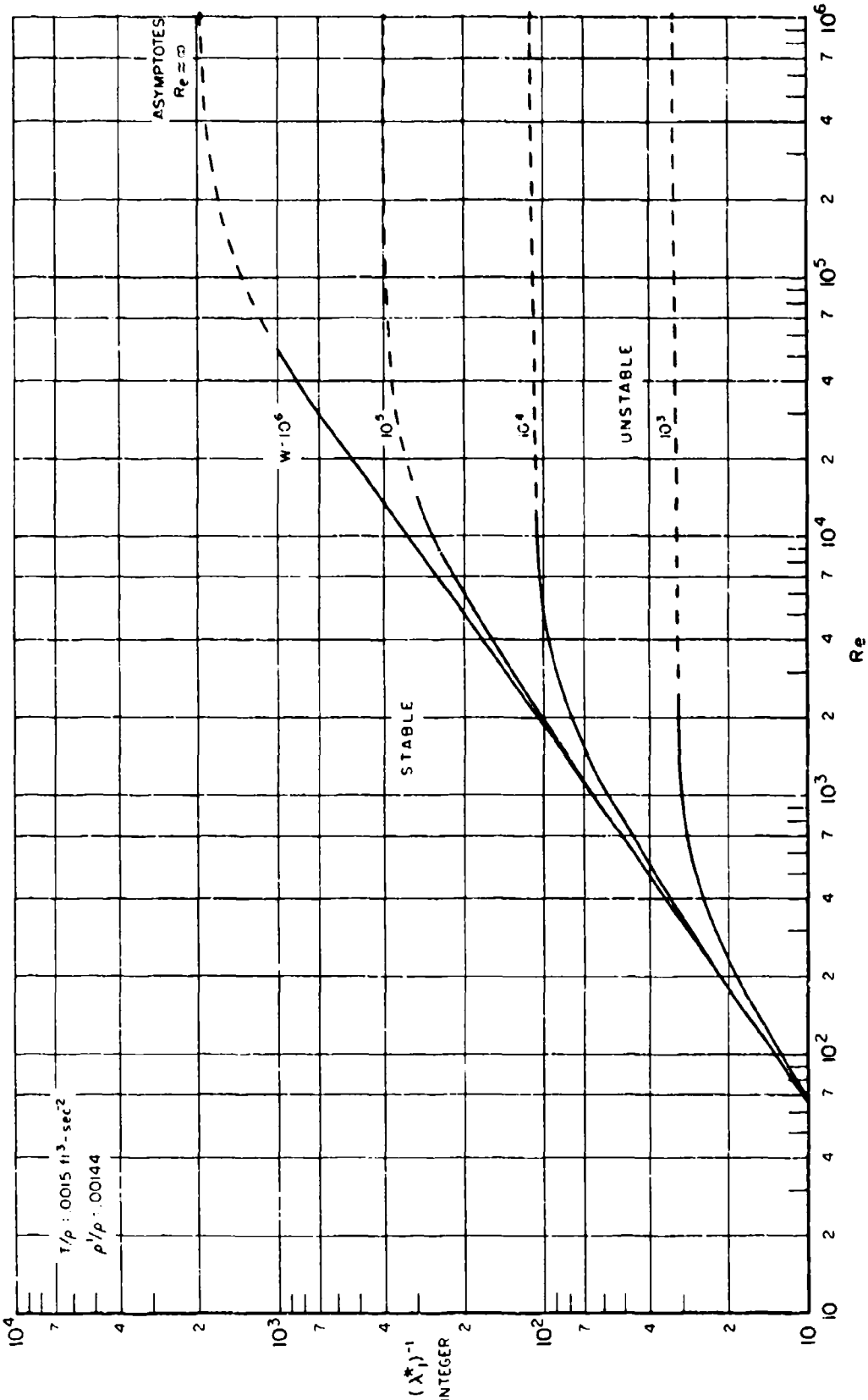

FIG. 7: STABILITY BOUNDARIES AS A FUNCTION OF REYNOLDS NUMBER AND WEBER NUMBER FOR A VISCOUS FLOW AND LARGE FILM THICKNESS

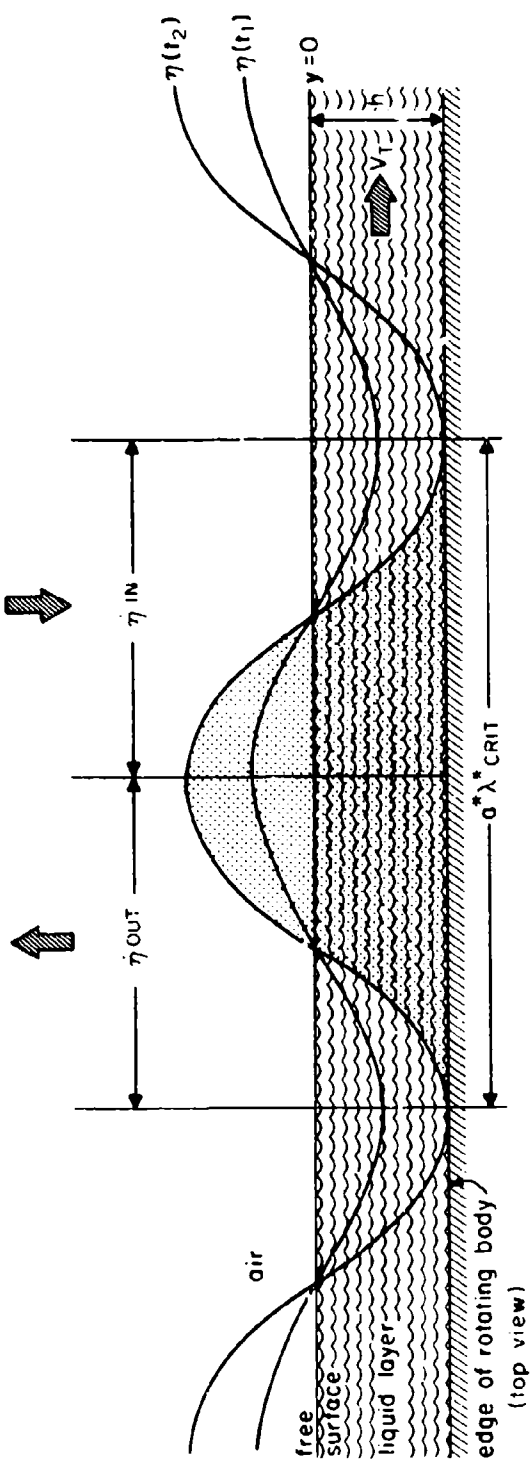

FIG. 8: SCHEMATIC OF FREE-SURFACE DIVERGENCE

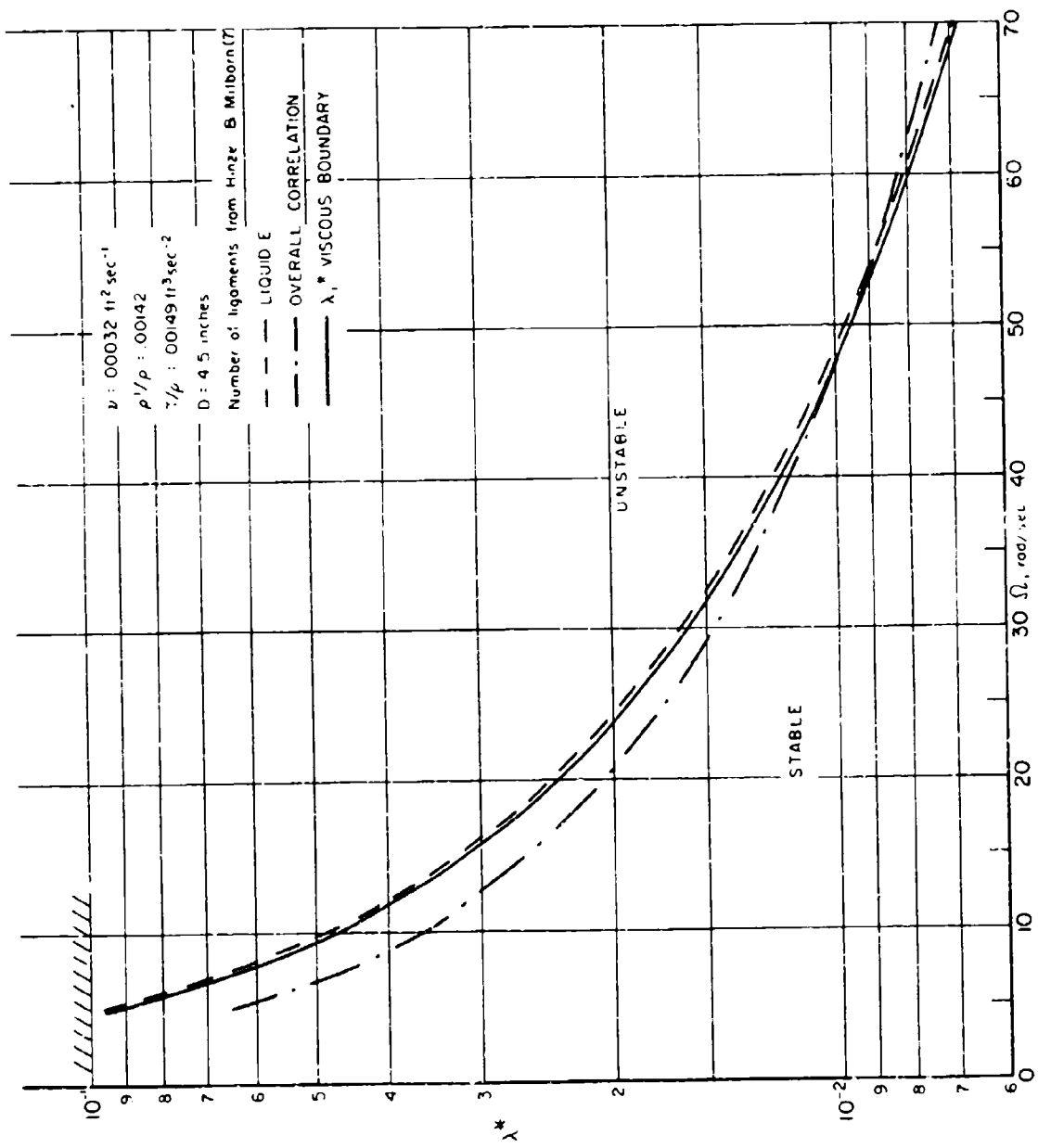

FIG. 9: CORRELATION OF THEORY AND EXPERIMENT (HINZE AND MILBORN, REF 7)

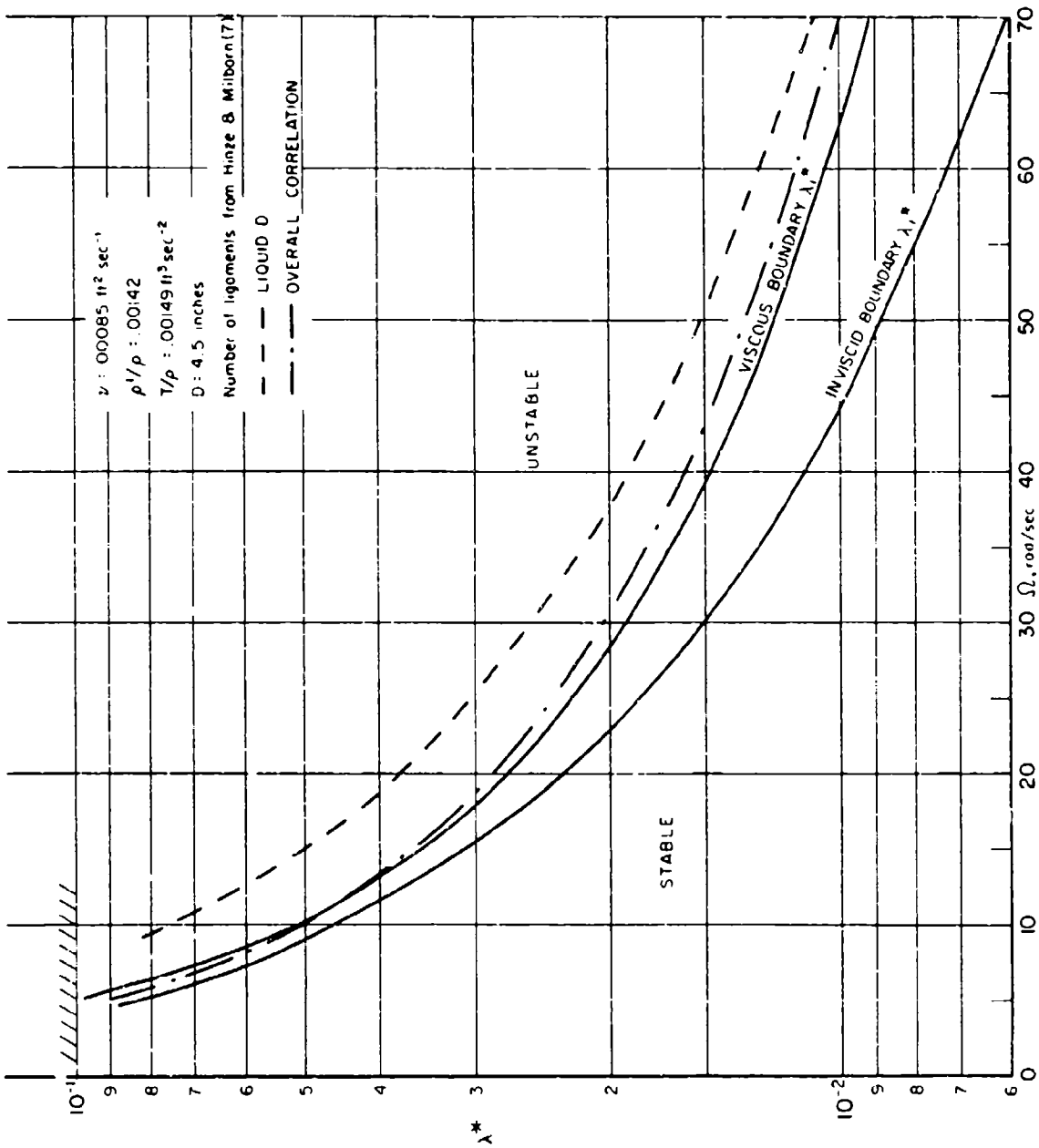

FIG. 10: CORRELATION OF THEORY AND EXPERIMENT (HINZE AND MILBORN, REF 7)

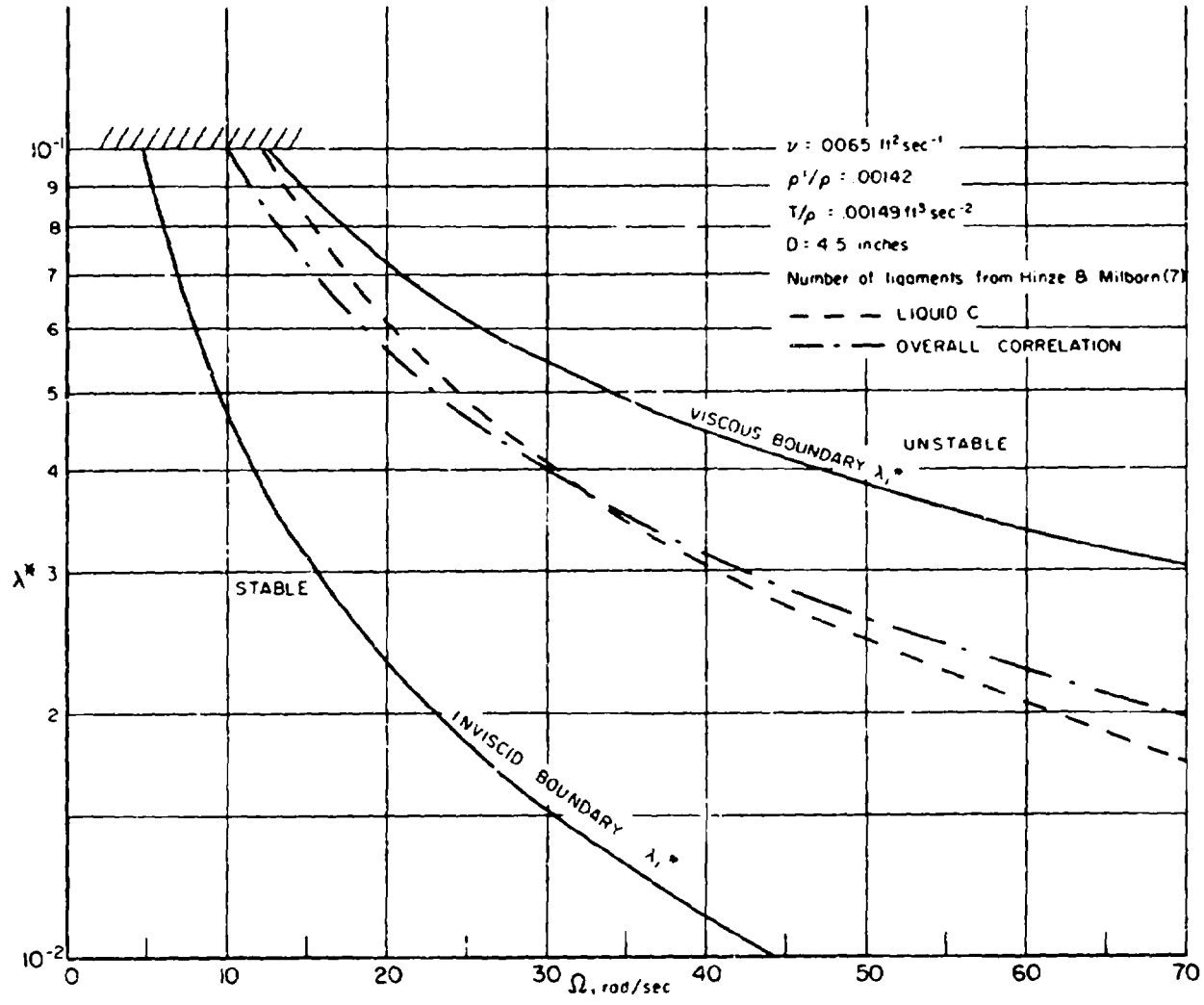

FIG.11: CORRELATION OF THEORY AND EXPERIMENT (HINZE AND MILBORN, REF 7)